Computational Approaches for the Designing of Novel Anticancer Compounds Based on Pyrazolo[3,4-d]pyrimidine Derivatives as TRAP1 Inhibitor

Amena Ali
Taif University College of Pharmacy https://orcid.org/0000-0001-8463-5182
Ola AbuAli
Taif University College of Science https://orcid.org/0000-0003-0785-5725
magda abdellattif (m.hasan@tu.edu.sa)
Taif University College of Science https://orcid.org/0000-0002-8562-4749

Research article

Keywords: 3-D QSAR, ADME, TRAP1 kinase, Docking, Enumeration, Virtual screening, TRAP1

Posted Date: October 26th, 2020

DOI: https://doi.org/10.21203/rs.3.rs-94143/v1

Abstract

Tumor necrosis factor (TNF) receptor associated protein 1 (TRAP1), a mitochondrial paralog of Heat Shock Protein (Hsp90), is associated with tumorigenesis promotion in different cancers through the maintenance of integrity of mitochondria, reprogramming cellular metabolism and reducing the production of reactive oxygen species (ROS). Therefore, both TRAP1 and Hsp90 are found to be of interest as targeted in the development of cancer therapeutics. In the current research, various computational approaches have been used in the development of TRAP1 inhibitors as anticancer compounds of Pyrazolo[3,4-d]pyrimidine derivatives. The various studies including development of pharmacophore, docking, 3-D QSAR, virtual screening and other studies were performed on 34 different Pyrazolo[3,4-d]pyrimidine derivatives to record the potential ability of these compounds. The required key features for the study is being provided by the pharmacophore study which provide DHHRR_1 hypothesis. 3D QSAR (atom-based analysis) was performed with different 34 pyrazole derivatives, which has been divided into two groups i.e. training set and test sets, provide the knowledge of the involvement of various fields of atom-based QSAR. The statistically significant model for this QSAR model was determined by partial least squares regression (PLS) method for which R^2 =0.96 and Q^2 = 0.57 would be considered significant. The LOO cross-validation R2 CV = 0.58 was used for the validation of QSAR model. Based on the virtual screening study protocol for the optimized binding interaction with **TRAP1** kinase receptors (PDB ID: **5Y3N**), the compounds ZINC05297837, ZINC05434822 and ZINC72286418 were produced. The maximum XP docking scores (-11.265, -10.532, -10.422, -10.827, -10.753) were observed for potent pyrazole analogues (42, 46, 49, 56, 43) by docking study representing their possible significant interactions with amino acid residues (ASP 594, CYS 532, PHE 583, SER 536). Absorption, distribution, metabolism, and excretion (ADME) analysis was carried out providing the key information for the newly designed compounds and their drug ability. The results of the docking study were correlated with the 3-D QSAR analysis revealed the active conformation of TRAP1 inhibitors which is helpful and important for activity performance with future perspective.

1. Introduction

TRAP1 is a 90 kDa mitochondrial paralog Hsp90 and bioenergetic regulator which is closely related to the tumorigenesis promotion in a variety of cancers [1,2]. TRAP1 helps in the maintenance of mitochondrial integrity, thus smooths the progression of a cell death against cellular stresses which is obtained by reduced ROS production along with reprogramming cellular metabolism. These two factors make cancer cells to get better adaptation in the harsh tumor microenvironments [3-5]. TRAP1 inactivation encourages cancer cells to undergo substantial apoptosis, *in-vitro* and *in-vivo*, hence numerous targeting mitochondrial TRAP1 inhibitors have been developed [6].

TRAP1 is an imperative bioenergetic regulator due its ability to inhibit both cytochrome oxidase and succinate dehydrogenase (SDH) [7-9]. TRAP1 also have the ability to provide resistance to oxidative stress [9] and counterbalance permeability of mitochondrial transition and consequent cell death.

In the present work, attempts have been made to carry the computational analysis for the different 34 pyrazole analogues, as reported in literature. 3-D pharmacophore mapping was used in order to identify the important pharmacophoric features accountable for biological activity. The role of individual atom contributing in the model development was basically based on the atom-based model development. The virtual screening studies provide the information about the potential effects of various ZINC compounds against the TRAP1 which are comparable to dataset. The important molecular interactions with the TRAP1 active site were studies by molecular docking studies for the various surrounded amino acids. The novel effective inhibitors of TRAP1 target was determined by using various computational approaches, like pharmacophore mapping, 3-D QSAR, virtual screening and molecular docking which provide the harmonizing information to support the development of potent inhibitors.

2. Materials And Methods

2.3 Pharmacophore hypothesis generation Relation between the chemical features and structural similarities for mentioned 34 compounds provide the chance of generation of possible 20 hypotheses which explain the binding ability of active molecules with receptors, having box size of 1 Å with 2 Å minimum inter site distance. The features up to 5 were set helping in generation of maximum variants supporting in the establishment of common pharmacophore hypothesis [18]. The different parameters for the pharmacophore hypotheses include: (1) Phase hypothesis score: rank-orders a new scoring function hypotheses helpful in providing the knowledge of performance in virtual screening and quality of ligand alignment, provide easy recognition of multiple binding modes by training against diverse known actives through perception of common pharmacophore; (2) Site score: help in providing the intimacy of superimposition of site point to pharmacophore of the structure; (3) Survival score: act as blending terms for the number of matches providing the relation between the relative energy and activity of the reference ligand; (4) Selectivity score: provide negative logarithm of part of molecules in the Index help in matching the hypothesis; (5) Average outranking: active adjusted rank minus one, outranking decoys are calculated for every docked active and then averaged; (6) Receiver operating characteristic (ROC): aid in data analysis as an indicator of model performance providing the demarcation of active site from inactive compounds; (7) Vector score: average cosine of the angles between the analogous pairs of vector features (donors, acceptors and aromatic rings) in different associated structures; (8) Active matched: give knowledge of number of active ligands matching the said hypothesis [19-22]. 2.4 Model developments by 3-dimensional QSAR study 2.4.1 Atom based QSAR Atom based 3-D QSAR model help in predicting the activities of other molecules. It was developed by Schrodinger Maestro v12.1 from a set of aligned ligands. The compounds have been divided in the ration of 70% and 30% in the training set and test set, respectively. The compounds clustering was carried by PLS factor of 5 [23, 24]. Table 3 summarized the different parameters of QSAR model which are as Factors: number of different factors for partial least squares regression model, SD: regression standard deviation, R2: value for regression, R2 CV: cross-validated R2 value calculated though the predictions acquired by a leave-N-out approach, F: Variance ratio, higher statistically significant regression are represented by larger F values, P: significance level of variance ratio, a greater degree of confidence are represented by smaller values, RMSE: root-mean-square error of the test set, Q2: for the predicted activities of test set, Pearson-R: for the predicted activities of the test set. Atom type fraction segment displayed the fraction due to each atom type in the QSAR model for each number of PLS factors used in the model. The confirmation of least diversity in the biological activities between molecules of training set through the scatter plot obtained by plotting actual activity against predicted activity [25, 26]. 2.4.2 Generation of Contour maps The contour maps help in predicting the favourably or unfavourably interaction of aligned molecules with the receptor for

biological activity and correspond to the spatial arrangement of aligned molecules. In Field based model, regions with favourable steric fields are represented by green contours and regions with unfavourable steric fields are represented by yellow contours. Moreover, the blue and red contours highlight the positions where electropositive groups and electronegative groups would be favourable, respectively. Thus, it is clear that biological activity will be greater when there is more steric bulk near green, less steric bulk near yellow, more positive charge near blue and more negative charge near red. Hydrogen bond donor contour map, donor bulk near purple is favourable, but the donor bulk near cyan is unfavourable for greater biological activity. For the hydrogen bond acceptor contour map, acceptor bulk near red is desired and acceptor bulk undesired near magenta for improved biological activity [27]. Whereas in Atom based model blue cubes represent increase in activity and red coloured cubes represent decrease in activity by a particular group. The contour maps have been described as follow: The atom-based 3-D QSAR model visual representation; (a) electron withdrawing, (b) hydrogen bond donor, (c) hydrophobic, (d) positive ionic where the positive coefficient (increase in activity) is represented as blue coloured cubes while negative coefficient (decrease in activity) is represented as red-coloured cubes represents. Field contour maps; (a) Electrostatic fields: blue as favoured electropositive and red as disfavoured electronegative. (b) Hydrogen bond acceptor field: red as favoured and magenta as disfavoured. (c) Hydrogen bond donor field: purple as favoured and cyan as disfavoured. (d) Steric field: green as favoured and yellow as unfavoured. 2.5 3-D QSAR model evaluation The 3-D QSAR model evaluation was carried out by taking key statistical parameters such as squared cross-validation coefficient (q2), squared non-cross-validation coefficient (r2) and predictive r2 (r2pred), standard error of estimate (SEE). The developed model was tested for internal quality which was based on the q2 value with an acceptance criterion of >0.5 statistically for significant model. The r2 provide the relative measure of the fit using regression equation whose value near to 1.0 illustrate the best fit of regression. Standard error of estimate is supportive in conveying the information about the variation of residuals or regression line [28, 29]. 2.6 Virtual screening studies on ZINC database The virtual screening study through ZINC database was performed by using pharmacophore hypothesis DHHRR_1 and most active compound 48 (Supplementary file S1). The ZINC database was used as drug like filters to download the 7543 molecules. The prediction of target was further performed by using Swiss Target Prediction which is a freely accessible tool for receptor database (Supplementary file S2) through which the target exploration become more convenient and useful. Swiss Target Prediction was used to predict the various protein targets among which the TRAP1 was the topmost suitable target for different molecules taken. Thus, the screening of molecules was further performed through molecular docking having standard and extra-precision mode against TRAP1 using GLIDE module of Schrodinger [30]. 2.7 Docking study Molecular docking studies on pyrazole analogues with TRAP1were carried out by using Glide module software (Schrodinger Maestro v12.1). Protein data bank (PDB ID:5Y3N) was used for determining the protein structure which were further processed through “protein preparation wizard” (Maestro wizard v12.1). Both, the generating states as well as refinement step were helpful in automatic addition of H atoms along with some important bonds at missing sites of protein molecule. The refinement step is crucial as it involve in the optimization of H bonded groups, dehydration and restrained minimization by using default force field OPLS_ 3e. The completion of optimization process was followed by processing of receptor grid to calculate binding pocket of receptors. Various docked ligand conformations were observed in docking results showing their binding energy scores. The ranking on the basis of scores were given representing high rank for lesser scoring conformation [31, 32]. 2.8 ADME property predictions ADME properties were determined by using Swiss ADME and Schrodinger ADME online tool helping in ligands selection with drug-like properties. Lipinski (Pfizer) filter: implemented as MW≤ 500, MLOGP ≤ 4.15, N or O ≤ 10, NH or OH ≤ 5 [43]. Ghose filter: implemented as 160 ≤ MW ≤ 480, -0.4 ≤ WLOGP ≤ 5.6, 40 ≤ MR ≤ 130, 20 ≤ atoms ≤ 70 [33-34]. Leadlikeness: implemented as 250 ≤ MW ≤350, XLOGP ≤3.5, Number of rotatable bonds ≤ 7; Synthetic accessibility: from 1 (very easy) to 10 (very difficult) [35]. Default settings were employed for these calculations. 2.9 Enumeration study R-group enumeration module of Schrödinger was implemented for R-group based enumeration of the Pyrazolo scaffold. Drug-Like filters like, REOS and PAIN’s series were used for separating the compound having reactive functional groups. The obtained drug-like compounds were further processed for preparation of ligand along with the minimum energy with the help of OPLS3e force field. Additionally, the docking of final screened compounds was performed in TRAP1 crystal structure in ligand-binding cavity through Glide SP protocol, resulting docking poses. From these different docking poses, best 50 poses were selected from different enumeration for further XP docking protocol providing the XP descriptors. This help in describing contribution of each atom in terms of penalties and rewards for docking energy. Enrichment calculations were performed for 1000 decoy compounds (from DUD.E database) and 30 Compounds (XP best poses) with the help of Schrodinger software while docking were performed by using XP protocol. The results obtained help in predicting validation of docking protocol as Receiver Operating Characteristic (ROC) curve demonstrate R2= 0.92.

3. Results And Discussion

3.1 Selection of best pharmacophore hypothesis

All the selected compounds (compounds 1 to 34) from the database were screened to get five probable common pharmacophore features from the list of variants i.e. 2 aromatic rings, 2 hydrophobic interaction, and 1 hydrogen bond donors. The mentioned features were supposed to have essential role in inhibitory ability of different compounds towards the target. Among the 20 hypotheses generated by PHASE module, DHHRR_1 hypothesis was considered to be best depending on a scoring function mentioned in **Table 2**.

3.2 Pharmacophore model evaluation

The pharmacophore model quality was calculated by using two evaluation tools i.e. percent screen plot & ROC plot. Percent screen plot represents the plot of the percentage of actives recovered and percentage of ligands screened for the hypothesis. ROC plot represents the plot between the true positive rate (sensitivity) and false positive rate (specificity) for various cutoff points. A test is considered to be perfect discrimination when it does not have any overlapping in two distributions and test has a ROC curve representing 100% specificity and 100% sensitivity by passing through the left upper corner. The more closely the position of curves in left upper corner represents the higher overall accuracy of the method. Both, percent screen plot as well as ROC plot was found to be an extreme left corner recommending the better accuracy of the generated hypotheses by PHASE module, as shown in **Fig 3 (A)** & **Fig 3 (B).**

3.3 Selection of atom based QSAR model

The QSAR results showed the important statistics of the fit for both test and training set. In table, each row shows the hypothesis results. Lines within each row is for regression models having a specific value for least squares factors and clustering compounds has been performed by PLS factor of 5. Different statistical parameters (SD, R^2, P, F, Q^2, RMSE and Pearson-R) in QSAR model was used taken in to account for reliable predictions and evaluation of QSAR model. The value of R^2 is required and high R^2 is essential for a model, but it alone does not provide the sufficient condition for ideal QSAR model prediction. Thus, predictive ability Q^2 values have to be chosen for best QSAR model prediction. Based on these parameters, five different models were developed by module and shown in **Table 3**. Among the five models, fifth model was found to be significant model owing to higher values of 0.57, 0.96 and 0.58 for Q^2, R^2& R^2 CV values, respectively. Though the higher value for SD (0.46) and RMSE (0.64) was recorded but very low values of 0.08, 0.34 and 0.08 for Q^2, R^2& R^2 CV values respectively eliminates the probability of first model selection. The required statics for atom-type fraction are reported in **Table 4**. Similarly, Table 5 represent the predicted pIC_{50}, actual pIC_{50} and residual values for generated models. The atom type fractions map provide the information of fractions of each atom of the training set affects the activity and is shown in **Fig. 4.** The uniform distribution of training set obtained by using scatter plot of displayed module passing through the origin (0, 0) as straight line is shown in Fig. 5.

3.5 Contour map analysis

Contour maps help in predicting the biological activity and its correlation with various substituents on the core moiety (**Fig. 4**) and help in determining the effect of adding substituent' on the biological activity. Increase in biological activity is represented by blue colour while decrease in biological activity is represented by red colour occlusion map. Among the 34 compounds, the most active compound was selected on the basis of high survival value of DHHRR_1 of atom-based 3-D QSAR contour maps. Increase in activity is accountable due to substitution of electron withdrawing group on phenyl ring attached to Pyrazolo[3,4-d]pyrimidine, suggesting that substitution of various groups like -CN, $-NO_2$, CF_3, $-NR_3$, -COR –X, etc on phenyl ring is answerable for augmented activity. Further, enhanced anticancer activity could be obtained by addition of hydrogen bond donor group at Pyrazolo[3,4-d]pyrimidine ring. Moreover, the hydrophobic group cover up the larger part of the ring and accountable for mixed activity.

3.6 Results of molecular docking

Molecular modelling was performed to examine the possible interactions between protein and most potent derivative through the comparative modelling by using the Schrodinger Glide module. The inhibition of enzyme activity depends on the possible interactions of inhibitors with various amino acid residues of targeted protein of interest. Docking was performed for all analogues to study the binding cavity of TRAP1 (**PDB ID: 5Y3N**) and are shown in **Fig.6 and Fig. 7.** The H-bond are shown by purple colour arrows and Π-Π stacking interactions are shown by purple green colour arrows. The possible bond interactions of compound 42 with amino acid residues PHE 201, GLY162, ASN119, ASP158, PHE205 and TRP231 has been observed in the study. Similarly, the derivative compound 49 (XP docking scores value is -11.353) found to have possible critical interactions with PHE 201, ASN119, ASP158 and PHE205 **(Supplementary file S3)**. Further, the binding interactions of compound 43 has been observed with PHE 201, ASP158, GLY162 and PHE205 while in compound 56 interactions with PHE201, GLY202 and ASP158 amino acids were detected. These interactions were essential for TRAP1 inhibitory activity.

3.7 Results of virtual screening

The virtual screening study has been performed by means of pharmacophore hypothesis DHHRR_1 utilizing ZINC database, resulting in the screening of total 2832 compounds with the help of Lipinski's rule of five. These screened compounds were further used in high throughput virtual Screening (HTVS) docking methodology. The best 20% compounds from HTVS were subjected to SP docking. Similarly, top 20% screened compounds from SP docking were further subjected to XP docking **(Supplementary file S4)**. Total 16 compounds were screened through SP docking in which top hits, namely ZINC05434822, ZINC72286418, ZINC05297837, ZINC59358929 and were found with docking scores -11.97, -10.73, -9.98, -9.88, respectively. These compounds were taken into consideration for the further study, as final ZINC compounds. These compounds were evaluated in terms of binding interaction energy by MMGBSA. Among these four compounds, ZINC05297837 showed interaction with amino acid residue PHE205, TRP231 and ASN171 *via* phenyl ring (**Fig. 8**) while the ZINC05434822 show interaction with PHE 201 and ILE161 in the same cavity as shown by crystal ligand (**Fig. 8**). The compound ZINC59358929 showed binding interactions with ASN119, PHE201, PHE 205 and TRP231 which is considered significant for showing activity while the compound ZINC72286418 showed significant interactions with ILE161, PHE201 and PHE205 (**Fig. 9**).

The binding pocket residues are found to be similar as were obtained from binding of active compounds 42, 46, 48, 49, 56 and crystal ligand. The docking simulation study was further validated by checking the RMSD value which should be less than 2 Å.

3.8 MMGBSA based rescoring

MMGBSA-based rescoring method was used for calculation of binding free energy for ligands and ZINC hit compounds ZINC05434822, ZINC72286418, ZINC05297837 and ZINC59358929 (complex with PDB ID: **5Y3N**) which provide very high binding free energy as dG bind = -58.2, -42.07, -59.752 and -48.2 kcal/ mol, respectively) (**Table 6**) **(Supplementary file S5)**.

3.9 Prediction of ADME properties

The ADME properties were determined by using Schrodinger ADME and Swiss ADME tool for obtaining best scoring of dataset and ZINC compounds and shown in **Table 7** to **12**. All compounds showed significant ADME properties, like number of hydrogen bond donor between 0-3, number of hydrogen bond acceptor 7, number of rotatable bond 4-9, like molecular weight were <500, and molar refractivity of about 125 and are considerable **(Supplementary file S6 and Supplementary file S7)**. Lipophilicity profile of selected compounds represented the lipophilic character along with the high GI absorption, but none of the said compounds possess the ability to cross blood brain barrier representing no toxicity of selected compounds. Compound ZINC72286418 was found to be

soluble as determined by solubility profile of ZINC derived compounds while others were moderately soluble in water. The synthetic convenience of all the compounds was in good range **(Supplementary file S5, S6, S7 & S8)**.

Optimization of novel ligands

The optimization and development of novel TRAP1inhibitors can be performed by using 3-D QSAR and molecular docking studies. Here, results obtained by 3-D QSAR study has been graphically represented as the structure activity relationships (SARs) of Pyrazolo[3,4-d]pyrimidine core with different possible substituent's (**Fig. 10)**

Analysis of R group enumeration

On the basis of optimized structure several derivatives have been enumerated through R group enumeration study of Schrodinger software. The compound structures have been described in Table 12 with their XP docking scores. These compounds are novel derivatives of Pyrazolo[3,4-d]pyrimidine having good docking scores.

4. Conclusion

In the present study, development of pharmacophore hypothesis, QSAR, virtual screening and enumeration study has been performed for determining the potential inhibitors against TRAP1. The best hypothesis generated was DHHRR_1, which has been taken for virtual screening study through ZINC database. The 3D QSAR study determines the best statistical values after many times trial by changing the training and test set molecules. The resultant contour maps determine the features such as electrostatic, hydrogen bond acceptor, hydrogen bond donor and positive ionic, participate in activity. The docking study of potent pyrazole analogues (42, 46, 49, 56, 43) showed highest XP docking scores (-11.265, -10.532, -10.422, -10.827, -10.753). Docking study showed the interactions with amino acids such as PHE 583, CYS 532, SER 536, ASP 594 important for activity. The ADME properties showed the important physicochemical properties of the molecules. The virtual screening study performed on ZINC database produced compounds ZINC05434822, ZINC72286418 and ZINC05297837 showed essential binding interaction with receptor **TRAP1** (PDB ID: **5Y3N**). Correlating the docking results with the 3D-QSAR analysis can get more potential compounds as **TRAP1** inhibitors. The enumeration on different positions of pyrazole analogues produced compounds with best docking score may be used as synthesis in research laboratory.

Abbreviations

3-D QSAR Three-dimensional Quantitative Structure Activity Relationship

PLS Partial Least Squares

q^2 Squared Cross-validation Co-efficient

r^2 Co-efficient of Regression

PDB Protein Data Bank

LOO Leave One Out

PHASE Pharmacophore Alignment and Scoring Engine

ADME Absorption Distribution Metabolism Excretion

TRAP1 TNF Receptor Associated Protein 1

Glide Grid-based Ligand Docking from Energetics

Declarations

a- Availability of data and materials

Data are available

b- Competing interests

The authors have no any conflict of interest

c- Funding

The Research is self-funded

d- Author contribution

- Amena suggested idea, performed, In-silico studies, and write the draft

- Magda interpreted the results obtained, she got a temporary license from Schrödinger software Finally and write the final form
- Dr. Ola performed English editing and arrangement of the manuscript

e- Acknowledgment

- Appreciated thanks are introduced to Taif University Researchers Supporting Project Number (TURSP-2020/91), Taif University, Taif, Saudi Arabia
- Appreciated thanks also are introduced to Schrödinger learning team work for their support

References

[1] S.J. Felts, B.A. Owen, P. Nguyen, J. Trepel, D.B. Donner, D.O. Toft, The hsp90-related protein TRAP1 is a mitochondrial protein with distinct functional properties. J. Biol. Chem. (2000), 275, 3305-3312.

[2] B.H. Kang, J. Plescia, T. Dohi, J. Rosa, S.J. Doxsey, D.C. Altieri, Regulation of tumor cell mitochondrial homeostasis by an organelle-specific Hsp90 chaperone network. Cell (2007), 131, 257-70.

[3] H.K. Park, J.E. Lee, J. Lim, D.E. Jo, S.A. Park, P.G. Suh, B.H. Kang, Combination treatment with doxorubicin and gamitrinib synergistically augments anticancer activity through enhanced activation of Bim. BMC cancer (2014), 14, 431.

[4] H.K. Park, J.E. Lee, J. Lim, B.H. Kang, Mitochondrial Hsp90s suppress calcium-mediated stress signals propagating from mitochondria to the ER in cancer cells. Mol. Cancer (2014), 13, 148.

[5] H.K. Park, J.H. Hong, Y.T. Oh, S.S. Kim, J. Yin, A.J. Lee, Y.C. Chae, J.H. Kim, S.H. Park, C.K. Park, M.J. Park, J.B. Park, B.H. Kang, Interplay between TRAP1 and Sirtuin-3 Modulates Mitochondrial Respiration and Oxidative Stress to Maintain Stemness of Glioma Stem Cells. Cancer research (2019), 79, 1369-1382.

[6] B.H. Kang, TRAP1 regulation of mitochondrial life or death decision in cancer cells and mitochondria-targeted TRAP1 inhibitors. BMB Rep. (2012), 45, 1-6.

[7] Marco Sciacovelli, Giulia Guzzo, Virginia Morello, Christian Frezza, Liang Zheng, Nazarena Nannini, Fiorella Calabrese, Gabriella Laudiero, Franca Esposito, Matteo Landriscina, Paola Defilippi, Paolo Bernardi, Andrea Rasola, The Mitochondrial Chaperone TRAP1 Promotes Neoplastic Growth by Inhibiting Succinate Dehydrogenase, Cell Metabolism, Volume 17, Issue 6, 2013, Pages 988-999.

[8] Soichiro Yoshida, Shinji Tsutsumi, Guillaume Muhlebach, Carole Sourbier, Min-Jung Lee, Sunmin Lee, Evangelia Vartholomaiou, Manabu Tatokoro, Kristin Beebe, Naoto Miyajima, Robert P. Mohney, Yang Chen, Hisashi Hasumi, Wanping Xu, Hiroshi Fukushima, Ken Nakamura, Fumitaka Koga, Kazunori Kihara, Jane Trepel, Didier Picard, and Leonard Neckers, Molecular chaperone TRAP1 regulates a metabolic switch between mitochondrial respiration and aerobic glycolysis, PNAS April 23, 2013 110 (17) E1604-E1612;

[9] Giulia Guzzo, Marco Sciacovelli, Paolo Bernardi, Andrea Rasola, Inhibition of succinate dehydrogenase by the mitochondrial chaperone TRAP1 has anti-oxidant and anti-apoptotic effects on tumor cells, Oncotarget. 2014; 5:11897-11908. https://doi.org/10.18632/oncotarget.2472

[10] Darong Kim, So-Yeon Kim, Dongyoung Kim, Nam Gu Yoon, Jisu Yun, Ki Bum Hong, Changwook Lee, Ji Hoon Lee, Byoung Heon Kang, Soosung Kang, Development of pyrazolo[3,4-d]pyrimidine-6-amine-based TRAP1 inhibitors that demonstrate in vivo anticancer activity in mouse xenograft models, Bioorganic Chemistry, Volume 101, 2020, 103901.

[11] J.T. Leonard, K. Roy, On selection of training and test sets for the development of predictive QSAR models, QSAR Comb. Sci. 25 (2006) 235.

[12] Ligprep, version 2.5, Schrödinger, LLC, New York, NY., 201223. Phase, version 4.4, Schrödinger, LLC, New York, NY., 2012

[13] Vivek Asati, Sanjay Kumar Bharti, Ashok Kumar Budhwani, 3D-QSAR and virtual screening studies of thiazolidine-2,4-dione analogs: Validation of experimental inhibitory potencies towards PIM-1 kinase, Journal of Molecular Structure, 1133, 2017, 278-293,

[14] Phase, version 4.4, Schrödinger, LLC, New York, NY., 2012

[15] S.L. Dixon, A.M. Smondyrev, E.H. Knoll, S.N. Rao, D.E. Shaw, R.A. Friesner, PHASE: a new engine for pharmacophore perception, 3D QSAR model development, and 3D database screening: 1. Methodology and preliminary results, J. Comput. Aided Mol. Des. 20 (2006) 647-71.

[16] M. Rajeswari, N. Santhi, V. Bhuvaneswari, Pharmacophore and virtual screening of JAK3 inhibitors, Bioinformation 10 (2014) 157-63.

[17] L. Crisan, A. Borota, A. Bora, L. Pacureanu, Diarylthiazole and diarylimidazole selective COX-1 inhibitor analysis through pharmacophore modeling, virtual screening, and DFT-based approaches, Struct. Chem. 30 (2019) 2311-26

[18] Phase 4.4 Quick Start Guide, Schrödinger, LLC, May 2013

[19] A.A. Sallam, W.E. Houssen, C.R. Gissendanner, K.Y. Orabi, A.I. Foudah, K.A. El Sayed, Bioguided discovery and pharmacophore modeling of the mycotoxic indole diterpene alkaloids penitrems as breast cancer proliferation, migration, and invasion inhibitors, Med. Chem. Comm. 4 (2013) 1360-69

[20] M.D. Hall, N.K. Salam, J.L. Hellawell, H.M. Fales, C.B. Kensler, J.A. Ludwig, G. Szakáes, D.E. Hibbs, M.M. Gottesman, Synthesis, activity, and pharmacophore development for isatinbeta- thiosemicarbazones with selective activity toward multidrug-resistant cells, J. Med. Chem. 52 (2009) 3191-3204

[21] M.K. Teli, G.K. Rajanikant, Pharmacophore generation and atom-based 3D-QSAR of Niso - propyl pyrrole-based derivatives as HMG-CoA reductase inhibitors, Org. Med. Chem. Lett. 2 (2012) 1-10.

[22] P. Kamaria, N. Kawathekar, Ligand-based 3D-QSAR analysis and virtual screening in exploration of new scaffolds as Plasmodium falciparum glutathione reductase inhibitors, Med. Chem. Res. 23 (2013) 25-23

[23] A. Golbraikh, A. Tropsha, Predictive QSAR modeling based on diversity sampling of experimental datasets for the training and test set selection, J. Comput. Aid. Mol. Des. 16 (2002) 357-369

[24] O.P. Tanwar, R. Saha, M.M. Alam, M. Akhtar, 3D-QSAR of amino-substituted pyrido [3,2B] pyrazinones as PDE-5 inhibitors. Med Chem Res. doi: 10.1007/s00044-010-9523-y

[25]http://gohom.win/ManualHom/Schrodinger_20152_docs/maestro/help_Maestro/phase/atom_based_qsar.html

[26] P. Kirubakaran, K. Muthusamy, K.H. Singh, S. Nagamani, Ligand-based pharmacophore modeling; atom-based 3D-QSAR analysis and molecular docking studies of phosphoinositide-dependent kinase-1 inhibitors, Indian J. Pharmaceut. Sci. 74 (2012) 141-51

[27] A. Dixit, S.K. Kashaw, S. Gaur, A.K. Saxena, Development of CoMFA, advance CoMFA and CoMSIA models in pyrroloquinazolines as thrombin receptor antagonist, Bioorg. Med. Chem. 12 (2004) 3591-98

[28] M.G. Shinde, S.J. Modi, V.M. Kulkarni, QSAR and molecular docking of phthalazine derivatives as epidermal growth factor receptor (EGFR) inhibitors, J. Appl. Pharm. Sci. 7 (2017) 181-91

[29] M. Clark, R.D. Cramer III, N. Van Opdenbosch, Validation of the general purpose Tripos 5.2 force field, J. Comp. Chem. 10 (1989) 982-1012

[30] Kaushik AC, Kumar S, Wei DQ and Sahi S (2018) Structure Based Virtual Screening Studies to Identify Novel Potential Compounds for GPR142 and Their Relative Dynamic Analysis for Study of Type 2 Diabetes. Front. Chem. 6:23. doi: 10.3389/fchem.2018.00023

[31] Protein preparation wizard Schrödinger, LLC, New York, NY., 2012

[32] W.L. Jorgensen, D.S. Maxwell, J. Tirado-Rives, Development and testing of the OPLS all atom force field on conformational en ergetics of organic liquids, J. Am. Chem. Soc. 118 (1996) 11225-36

[33] C.A. Lipinski, F. Lombardo, B.W. Dominy, P.J. Feeney, Experimental and computational approaches to estimate solubility and permeability in drug discovery and development settings, Adv. Drug Deliv. Rev. 23 (1997) 3-25

[34] A.K. Ghose, V.N. Viswanadhan, J.J. Wendoloski, A knowledge-based approach in designing combinatorial or medicinal chemistry libraries for drug discovery. 1. A qualitative and quantitative characterization of known drug databases, J. Comb. Chem. 1 (1999) 55-68

[35] S.J. Teague, A.M. Davis, P.D. Leeson, T. Oprea, The design of leadlike combinatorial libraries, Angew Chem. Int. Ed. 38 (1999) 3743-8

Tables

Table 1: Different substituent of common core with biological activities in terms of IC50 & pIC50 values

R_1	Compounds	R	IC_{50} (nM)	pIC_{50}
1	4.00		0.50	6.30
2	9.00		19.00	4.72
3	10.00		7.00	5.15
4	11.00		15.00	4.82
5	12.00		20.00	4.70
6	13.00		20.00	4.70
7	15.00		20.00	4.70
8	22.00		6.50	5.19
9	23.00		5.00	5.30
10	24.00		20.00	4.70
11	25.00		4.00	5.40
12	26.00		20.00	4.70
13	27.00		3.50	5.46
14	30.00		20.00	4.70
15	32.00		15.00	4.82
16	33.00		20.00	4.70
17	34.00		4.00	5.40
18	35.00		10.00	5.00
19	36.00		8.00	5.10
20	39.00		3.00	5.52
21	41.00		1.23	5.91
22	42.00		0.44	6.36
23	43.00		2.43	5.61
24	44.00		1.80	5.74
25	45.00		1.69	5.77
26	46.00		0.47	6.33
27	47.00		1.98	5.70
28	48.00		0.37	6.43
29	49.00		0.89	6.05
30	50.00		0.94	6.03
31	51.00		0.79	6.10
32	52.00		0.45	6.35
33	56.00		2.70	5.57
34	59.00		1.00	6.00

Table 2: Different Pharmacophore hypothesis generated by the using of compounds and their activity

HypoID	Survival	Site	Vector	Volume	Select	Matches	Inactive	Adjusted	BEDROC	RefLig
DHHRR_1	5.94	0.93	1.00	0.91	2.15	9.00	2.66	3.28	1.00	mol_32
DHHRR_2	5.94	0.93	1.00	0.91	2.15	9.00	2.62	3.33	1.00	mol_32
DHHRR_3	5.94	0.93	1.00	0.91	2.15	9.00	2.68	3.26	1.00	mol_32
DHHRR_4	5.94	0.92	1.00	0.91	2.15	9.00	2.70	3.24	1.00	mol_32
DHHRR_5	5.94	0.93	1.00	0.91	2.15	9.00	2.63	3.30	1.00	mol_32
DHHRR_6	5.94	0.93	1.00	0.91	2.15	9.00	2.70	3.24	1.00	mol_32
DHHRR_7	5.93	0.92	1.00	0.91	2.15	9.00	2.75	3.19	1.00	mol_32
DHHRR_8	5.93	0.92	1.00	0.91	2.15	9.00	2.65	3.29	1.00	mol_32
DHHRR_9	5.93	0.93	1.00	0.91	2.14	9.00	2.64	3.29	1.00	mol_32
DHHRR_10	5.93	0.93	1.00	0.91	2.14	9.00	2.67	3.26	1.00	mol_32
DHRR_1	5.40	0.99	1.00	0.94	1.52	9.00	2.90	2.50	1.00	mol_26
DHRR_2	5.40	0.99	1.00	0.94	1.52	9.00	2.90	2.50	1.00	mol_26
DHRR_3	5.39	0.99	1.00	0.94	1.51	9.00	2.89	2.50	1.00	mol_26
DHRR_4	5.39	0.99	1.00	0.94	1.51	9.00	2.91	2.48	1.00	mol_26
DHRR_5	5.39	0.99	1.00	0.94	1.51	9.00	2.90	2.49	1.00	mol_26
DHRR_6	5.39	0.99	1.00	0.94	1.51	9.00	2.89	2.50	1.00	mol_26
DHRR_7	5.39	0.99	1.00	0.94	1.51	9.00	2.91	2.48	1.00	mol_26
DHRR_8	5.39	0.99	1.00	0.94	1.50	9.00	2.90	2.48	1.00	mol_26
DHRR_9	5.39	0.99	1.00	0.94	1.50	9.00	2.90	2.48	1.00	mol_31
DHRR_10	5.38	0.99	1.00	0.94	1.50	9.00	2.91	2.47	1.00	mol_31

Table 3: Statistical data of Atom-based QSAR model

# Factors	SD	R^2	R^2 CV	R^2 Scramble	Stability	F	RMSE	Q^2	Pearson-r
1.00	0.46	0.34	0.08	0.31	0.93	11.80	0.64	0.08	0.47
2.00	0.33	0.68	0.22	0.51	0.73	23.90	0.52	0.29	0.59
3.00	0.23	0.85	0.41	0.69	0.68	38.70	0.47	0.42	0.67
4.00	0.16	0.93	0.57	0.76	0.71	70.50	0.41	0.56	0.76
5.00	0.13	0.96	0.58	0.81	0.70	82.50	0.40	0.57	0.79

Table 4: 3D-QSAR statistics for atom-type fraction

# Factors	H-bond donor	Hydrophobic/non-polar	Electron-withdrawing	Other
1	0.011	0.577	0.391	0.021
2	0.007	0.741	0.225	0.027
3	0.035	0.703	0.216	0.046
4	0.043	0.738	0.198	0.021
5	0.045	0.755	0.192	0.008

Table 5: Actual, predicted pIC_{50} and residual values of generated models

No^{r}	Name	Actual pIC_{50} (X)	Atom based	
			Predicted pIC_{50} (Ŷ)	Residuals (Ŷ -X)
1	4	6.3	6.00	-0.30
2	9	4.72	4.65	-0.07
3	10	5.15	5.76	0.61
4	11	4.82	4.85	0.03
5	12	4.7	4.66	-0.04
6	13	4.7	4.69	-0.01
7	15	4.7	4.68	-0.02
8	22	5.19	5.20	0.01
9	23	5.3	5.30	0.00
10	24	4.7	4.85	0.15
11	25	5.4	5.29	-0.11
12	26	4.7	4.67	-0.03
13	27	5.46	5.60	0.14
14	30	4.7	4.92	0.22
15	32	4.82	4.88	0.06
16	33	4.7	4.63	-0.07
17	34	5.4	5.46	0.06
18	35	5	4.89	-0.11
19	36	5.1	5.14	0.04
20	39	5.52	5.57	0.05
21	41	5.91	5.98	0.07
22	42	6.36	6.39	0.03
23	43	5.61	5.73	0.12
24	44	5.74	5.85	0.11
25	45	5.77	5.75	-0.02
26	46	6.33	6.11	-0.22
27	47	5.7	5.86	0.16
28	48	6.43	5.85	-0.58
29	49	6.05	6.02	-0.03
30	50	6.03	5.80	-0.23
31	51	6.1	6.11	0.01
32	52	6.35	6.20	-0.15
33	56	5.57	5.63	0.06
34	59	6	6.17	0.17

Table 6: Docking scores of active compounds and ZINC screened compounds with their MMGBSA scores

Compounds name	PDB ID:5Y3N		
	Docking score (xp) kcal/mol	Docking score (sp) kcal/mol	MMGBSA dG bind (xp complex) kcal/mol
48	**-10.824**	**-9.998**	78.07
42	-11.265	-11.265	-57.88
46	-10.532	-10.782	-56.71
49	-10.422	-11.353	-68.2
56	-10.827	-11.641	-82.07
43	-10.753	-11.508	-56.71
ZINC05434822	-11.63	-11.641	-68.2
ZINC72286418	-10.86	-10.59	-82.07
ZINC05297837	-10.42	-6.25	-59.752
ZINC59358929	-10.102	-9.68	-78.2

Table 7: ADME predictions of ZINC database and other active compounds

S. No.	Compounds Name	QP log Po/w	QPP Caco	QP logBB	QPPMDCK	#metab	QP logKhsa	Percent human oral absorption
1	48	**3.156**	920.499	-0.145	4124.662	1	0.106	100
2	42	2.644	1011.799	-0.193	2743.625	1	-0.039	96.212
3	46	2.972	1006.302	-0.295	2031.339	2	0.025	100
4	49	2.892	1037.573	-0.101	3427.589	1	0.027	100
5	56	2.686	1271.458	-0.292	1230.569	3	0.1	100
6	43	2.354	1053.419	-0.305	1260.235	2	-0.053	94.825
7	ZINC05434822	4.687	1015.224	-0.589	833.988	3	0.728	100
8	ZINC72286418	2.653	431.141	-0.802	581.552	3	0.1	89.635
9	ZINC05297837	2.728	258.436	-1.334	303.018	2	0.003	86.094

Table 8: Physicochemical properties prediction of ZINC database and other active compounds

S. No.	Name	Mol. Wt. (g/mol)	No. rot. bonds	No. H-bond acceptor	No. H-bond donors	Molar refractivity
1	48	356.58	2	4	1	78.14
2	42	429.6	2	5	1	89.27
3	46	325.7	3	6	1	76.89
4	49	313.67	2	6	1	70.36
5	56	376.21	2	5	1	89.17
6	43	317.73	2	5	1	81.52
7	ZINC05434822	363.43	5	4	1	102.8
8	ZINC72286418	334.29	5	5	2	80.71
9	ZINC05297837	469.29	5	5	3	118.83

Table 9: Lipophilicity profile ZINC database and other active compounds

S. No.	Compound name	Log $P_{o/w}$ (XLOGP3)	Log $P_{o/w}$ (WLOGP)	Log $P_{o/w}$ (MLOGP)
1	48	3.19	3.44	3.2
2	42	2.86	2.45	2.51
3	46	2.57	3.25	2.65
4	49	2.69	3.8	3.34
5	56	2.74	2.57	2.09
6	43	2.57	2.16	1.99
7	ZINC05434822	4.56	4.89	2.51
8	ZINC72286418	2.12	4.01	3.39
9	ZINC05297837	3.27	2.19	2.47

Table 10: Water solubility profile of ZINC database and other active compounds

S. No.	Compound name	Log S (ESOL)	Solubility (mg/ml)	Class
1	48	-4.48	1.17E-02	3.28E-05
2	42	-4.68	9.02E-03	Moderately soluble
3	46	-3.78	5.34E-02	Soluble
4	49	-3.88	4.17E-02	Soluble
5	56	-4.25	2.12E-02	Moderately soluble
6	43	-3.8	5.02E-02	Soluble
7	ZINC05434822	-5.21	2.27E-03	Moderately soluble
8	ZINC72286418	-3.29	1.72E-01	Soluble
9	ZINC05297837	-5	4.72E-03	Moderately soluble

Table 11: Pharmacokinetics results of ZINC database and other active compounds

S. No.	Compound name	GI absorption	BBB permeant	CYP1A2 inhibitor	CYP2C19 inhibitor	CYP2C9 inhibitor	CYP2D6 inhibitor	CYP3A4 inhibitor
1	48	High	Yes	High	Yes	No	Yes	Yes
2	42	High	No	Yes	No	Yes	No	No
3	46	High	Yes	Yes	No	No	No	No
4	49	High	Yes	Yes	Yes	No	No	No
5	56	High	No	Yes	No	Yes	No	Yes
6	43	High	No	Yes	No	No	No	Yes
7	ZINC05434822	High	No	Yes	Yes	Yes	Yes	Yes
8	ZINC72286418	High	Yes	No	Yes	No	Yes	No
9	ZINC05297837	High	No	No	No	No	No	No

Table 12: Drug likeness, lead likeness and synthetic accessibility of all compounds

S. No.	Compound name	Drug-likeness			Lead-likeness; violation	Synthetic accessibility
		Lipinski rule; Violation	Ghose rule; Violation	Bioavailability score		
1	**48**	**0**	**0**	**0.55**	1	**2.22**
2	42	0	0	0.55	1	2.7
3	46	0	0	0.55	0	2.39
4	49	0	0	0.55	0	2.25
5	56	0	0	0.55	1	2.84
6	43	0	0	0.55	0	2.6
7	ZINC05434822	0	0	0.55	2	3.67
8	ZINC72286418	0	0	0.55	0	2.92
9	SORAFENIB	0	0	0.55	1	3.37

Table 13: R group determination by enumeration study of Schrodinger software

Comp. name	Structure	XP GScore (PDB ID:5Y3N)	R1 s m smiles	R2 s m smiles	R3 s m smiles
1	O=C(C)Nc(n1)nc([NH+](C)C)c(c12)cnn2Cc(c(c3)C(=O)N)cc(c34)OCO4	-13.286	[*][NH+](C)C	[*]NC(=O)C	[*]C(=O)N
2	n1c([NH3+])nc(O)c(c12)cnn2Cc(c(c3)C(=O)N)cc(c34)OCO4	-13.286	[*]O	[*][NH3+]	[*]C(=O)N
3	C1C[NH2+]CCC1c(nc(n2)C(=O)N)c(c23)cnn3Cc(c(c4)C(=O)N)cc(c45)OCO5	-12.873	[*]C1CC[NH2+]CC1	[*]C(=O)N	[*]C(=O)N
4	NC(=O)c(n1)nc(O)c(c12)cnn2Cc(cc(c34)OCO4)c(c3)C(=O)Nc5ccccc5	-12.73	[*]O	[*]C(=O)N	[*]C(=O)Nc1ccccc
5	NC(=O)c(n1)nc(O)c(c12)cnn2Cc(cc(c34)OCO4)c(c3)-c5[nH]ccn5	-12.674	[*]O	[*]C(=O)N	[*]c1ncc[nH]1
6	NC(=O)c(n1)nc(O)c(c12)cnn2Cc(cc(c34)OCO4)c(c3)-c5[nH]cnc5	-12.622	[*]O	[*]C(=O)N	[*]c1cnc[nH]1
7	CNC(=O)Nc(n1)nc(O)c(c12)cnn2Cc(cc(c34)OCO4)c(c3)NC(=O)Nc5ccccc5	-12.608	[*]O	[*]NC(=O)NC	[*]NC(=O)Nc1cccc
8	n1c([NH3+])nc(O)c(c12)cnn2Cc(c(c3)C(=O)N(C)C)cc(c34)OCO4	-2.955	from water 1	15173	15183
9	c1nccn1-c(n2)nc(O)c(c23)cnn3Cc(cc(c45)OCO5)c(c4)C(=O)Nc6ccccc6	-12.559	[*]O	[*]n1ccnc1	[*]C(=O)Nc1ccccc
10	n1c([NH3+])nc([NH2+]C)c(c12)cnn2Cc(cc(c34)OCO4)c(c3)C(=O)Nc5ccccc5	-12.555	[*][NH2+]C	[*][NH3+]	[*]C(=O)Nc1ccccc

Figures

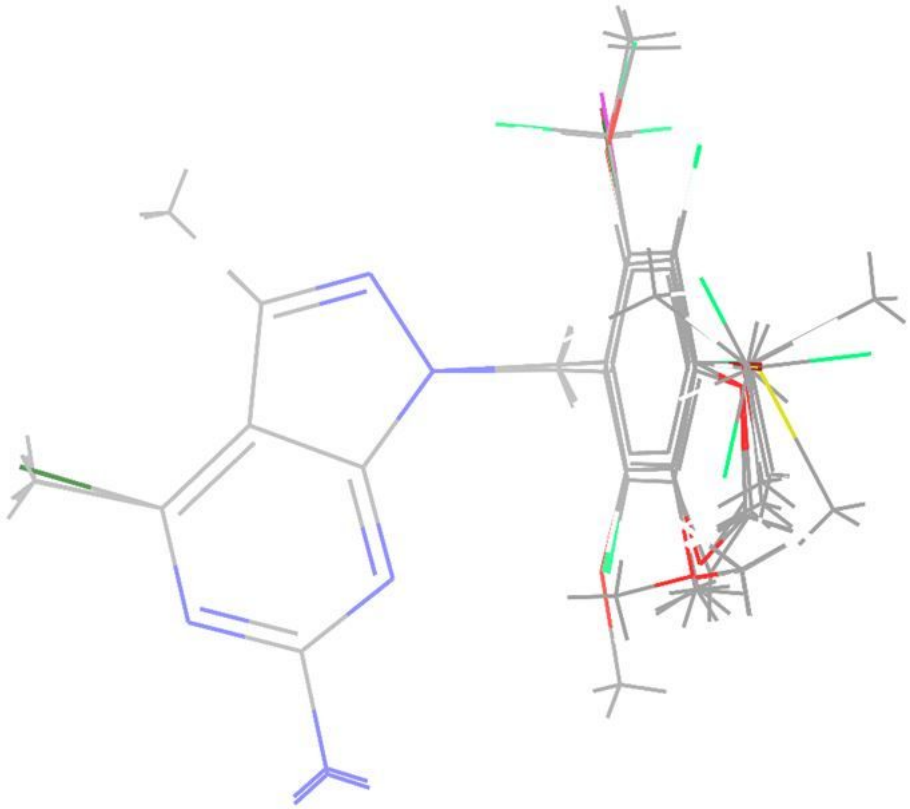

Figure 1

Alignment of common pharmacophoric features

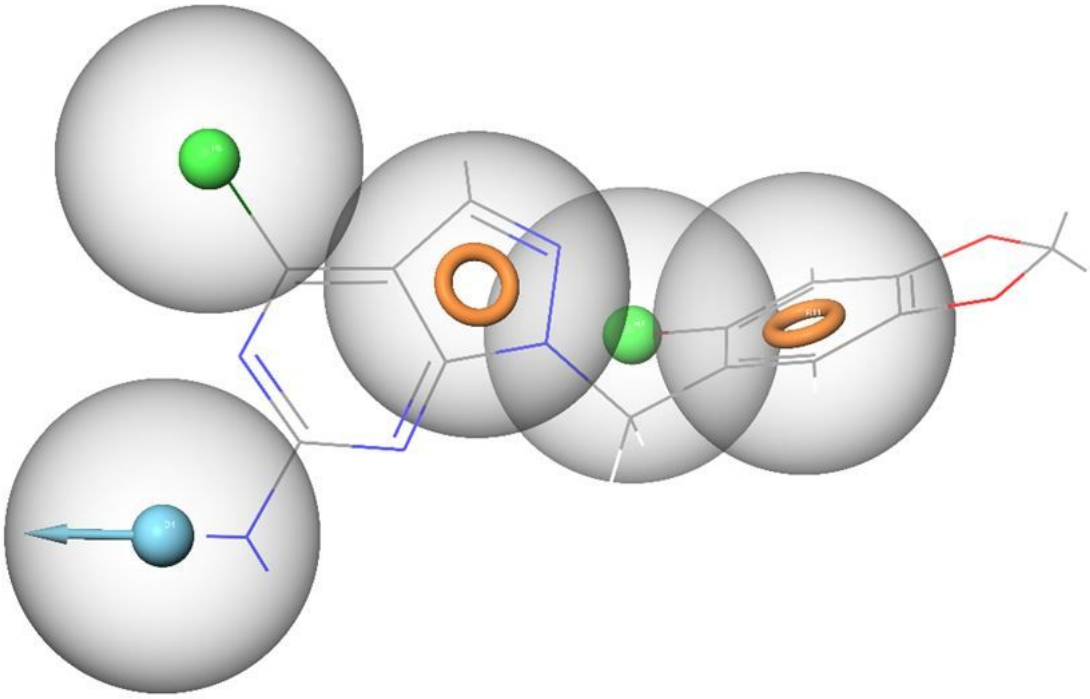

Figure 2

The best common pharmacophoric hypothesis

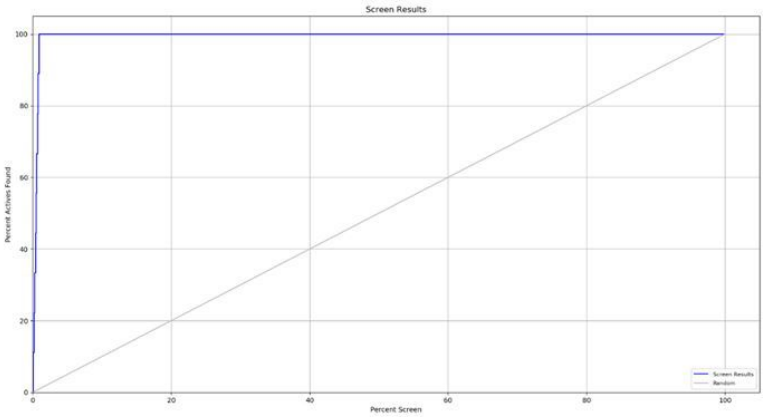

(A)

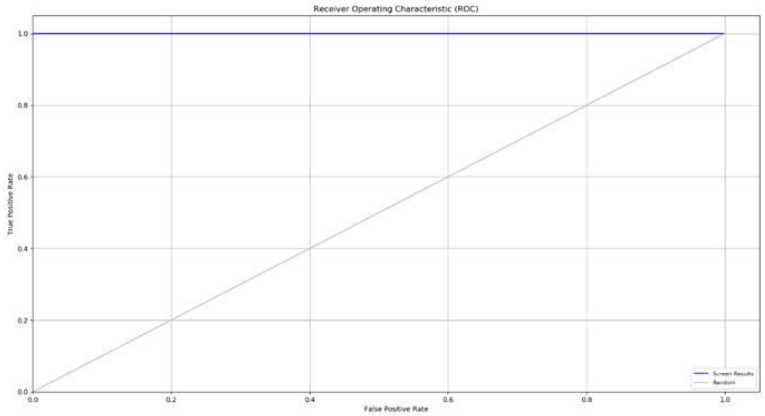

(B)

Figure 3

(A) Percent screen plot; (B) ROC plot

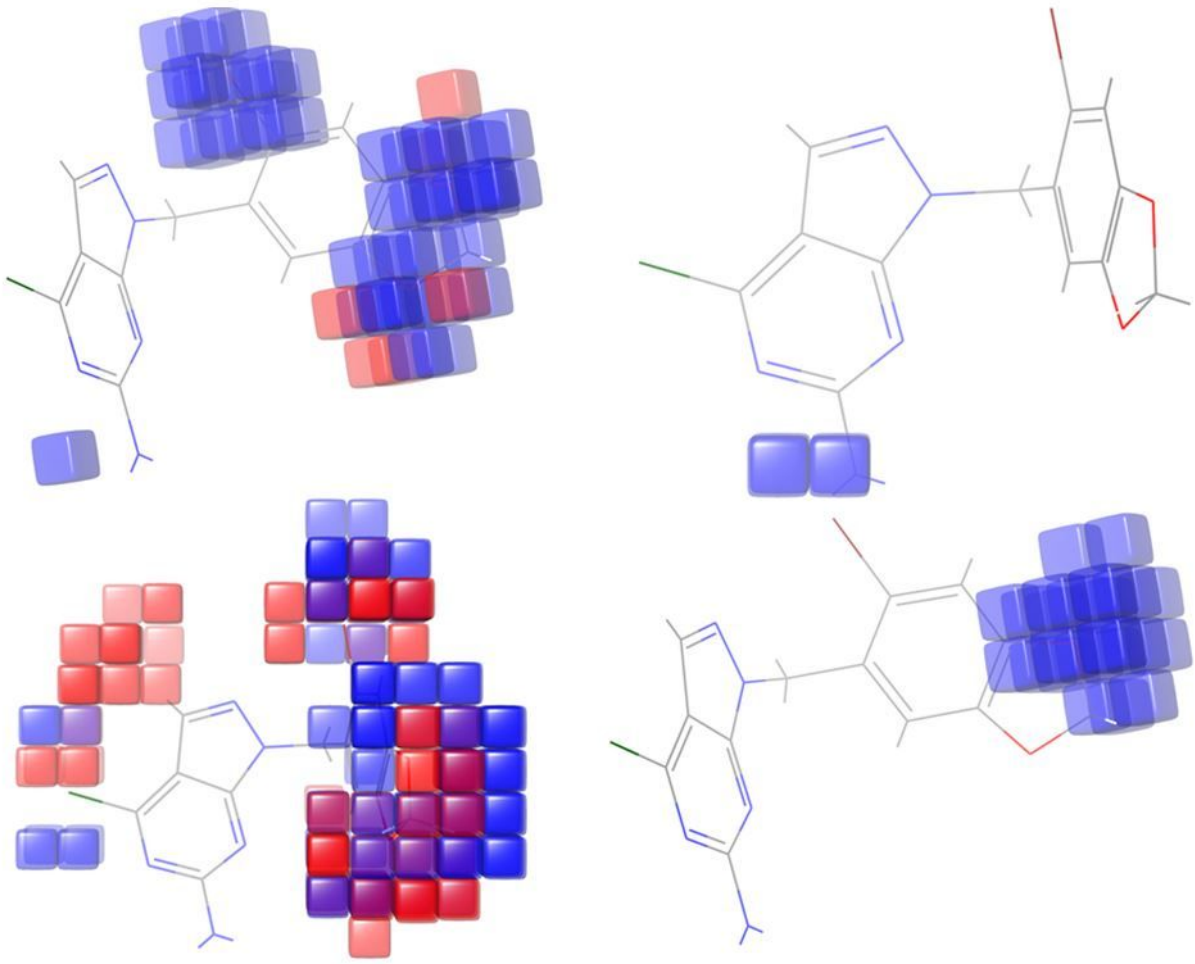

Figure 4

Atom-based 3D-QSAR model visual representation; (a) electron withdrawing, (b) hydrogen bond donor, (c) hydrophobic, (d) positive ionic where blue coloured cubes represents positive coefficient or increase in activity and red-coloured cubes represents negative coefficient or decrease in activity.

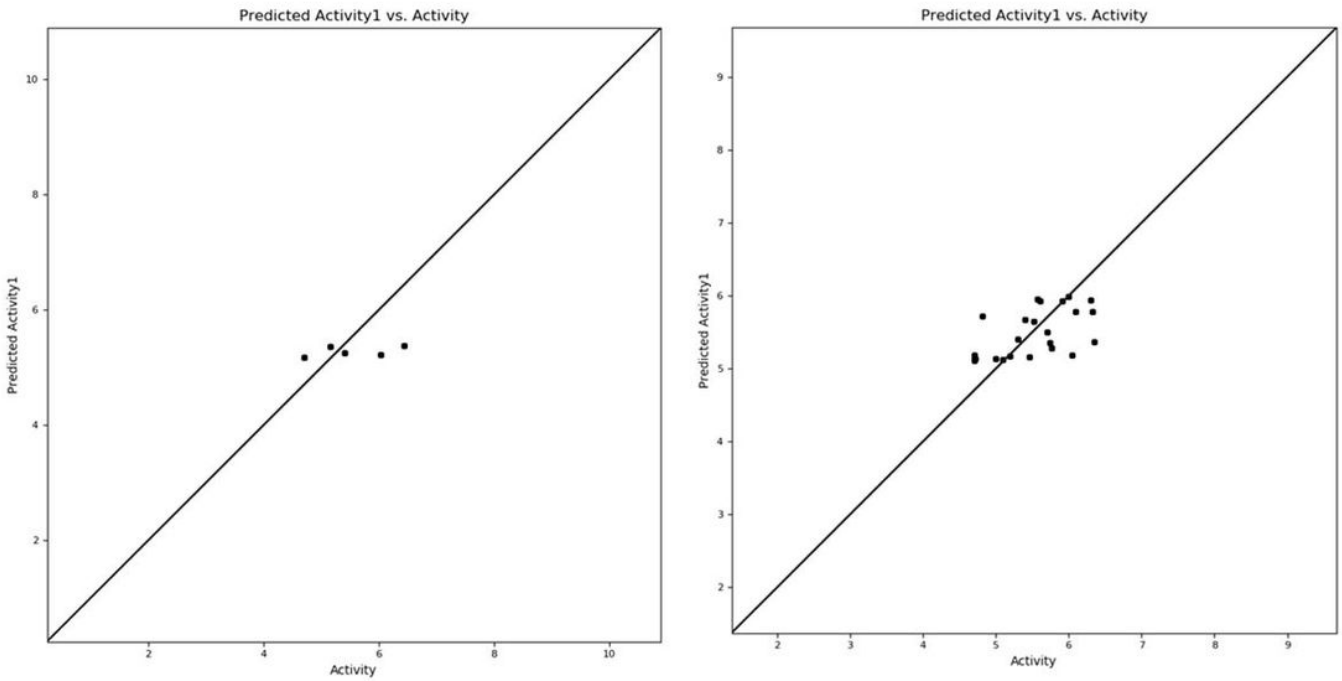

Figure 5

Represents the comparison between actual vs predicted pIC50 values of test and training set molecules, consecutively.

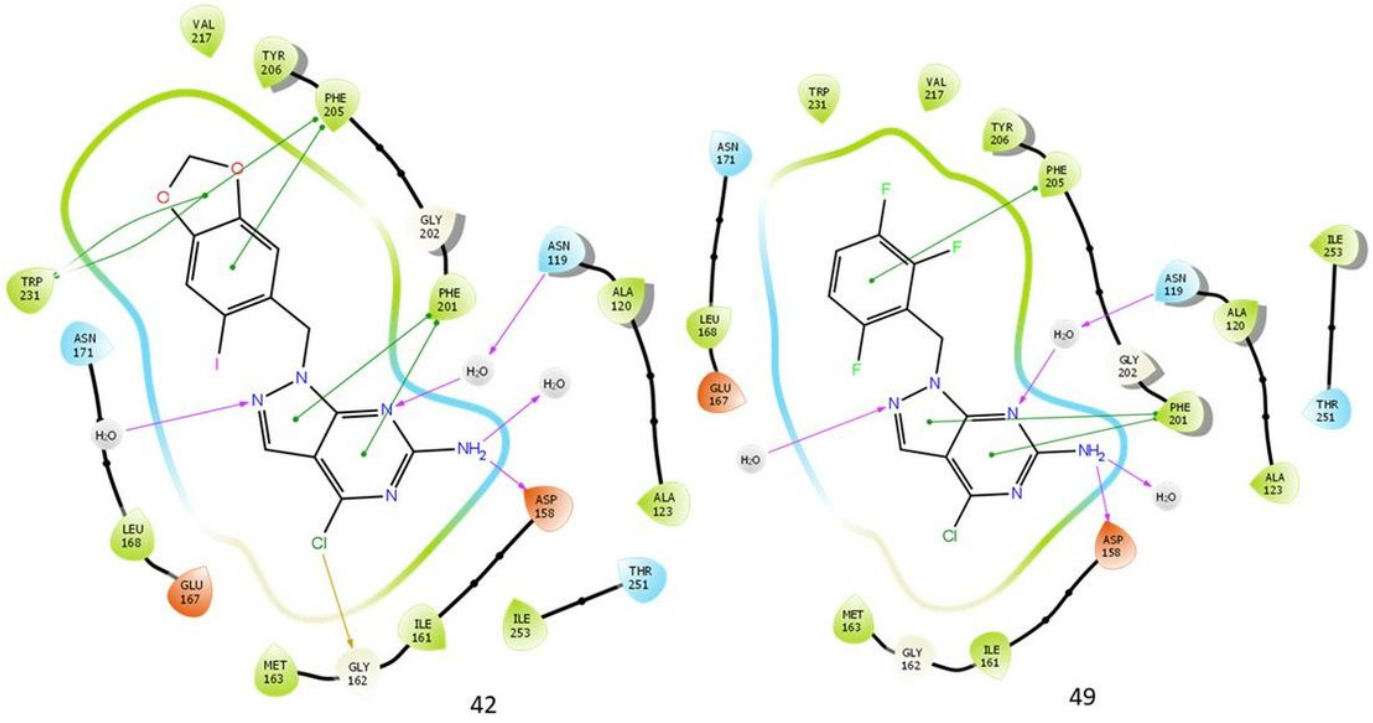

Figure 6

3-D and 2-D diagram showing binding interactions of compound 42, 49 with TRAP1 (PDB ID: 5Y3N)

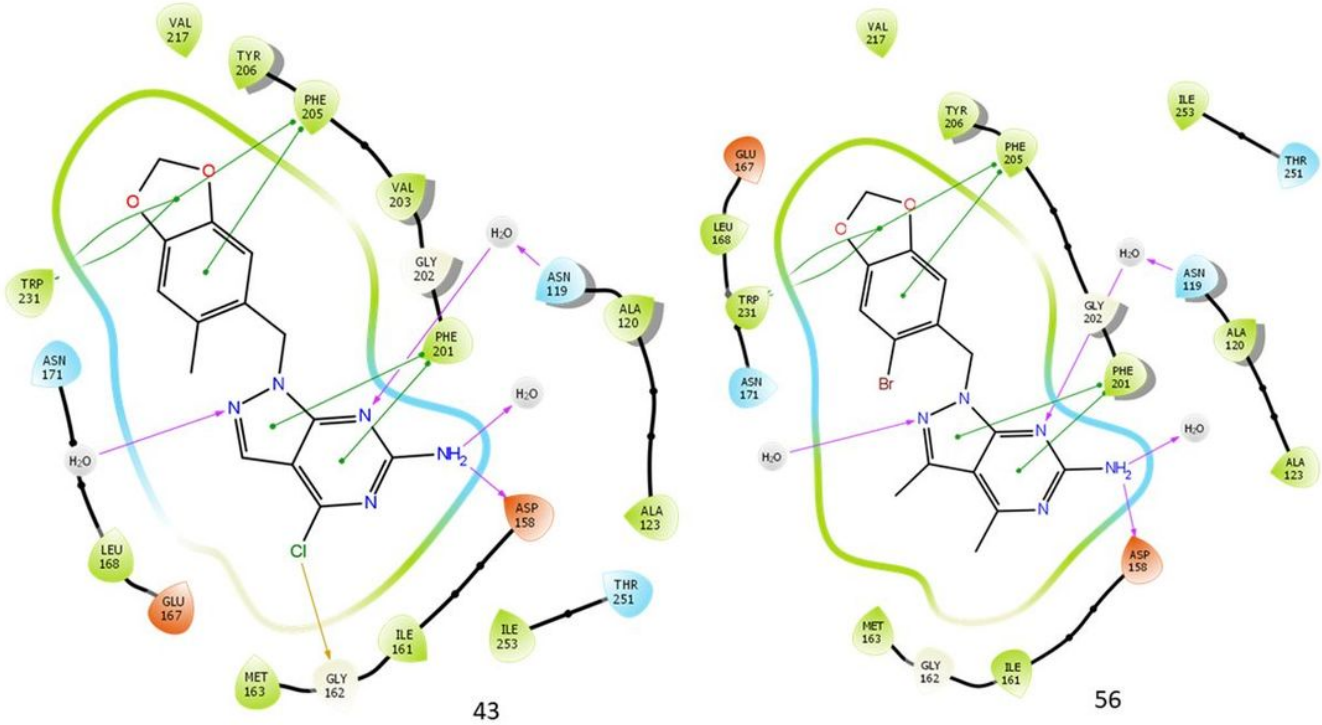

Figure 7

3-D diagram showing binding interactions of compounds43 and 56 with TRAP1 (PDB ID: 5Y3N)

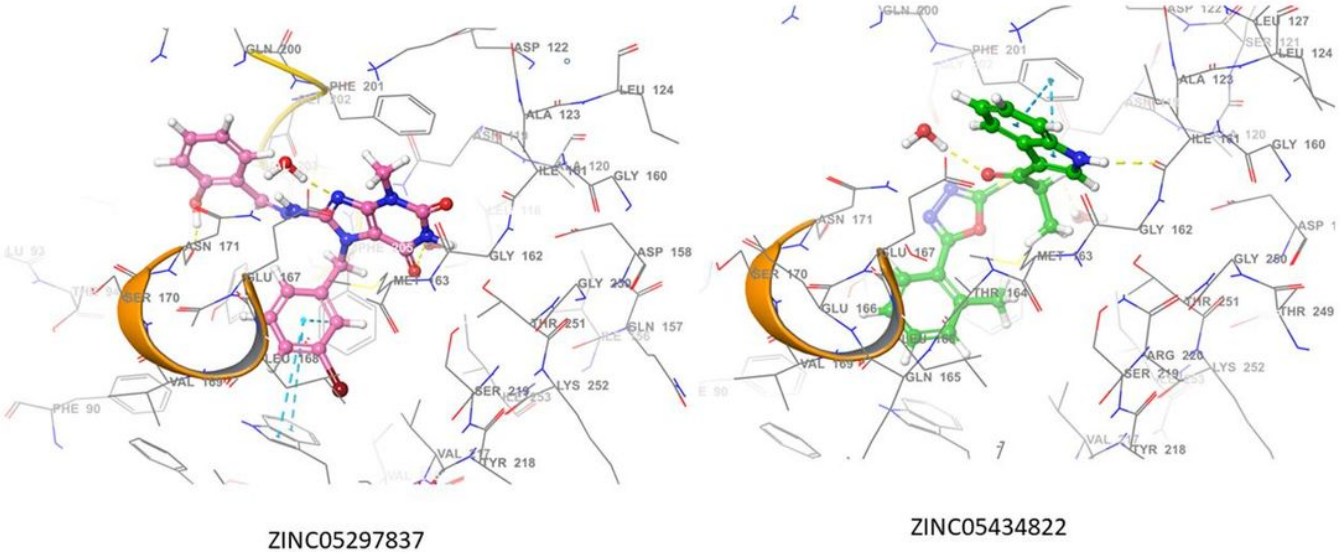

Figure 8

TRAP1(PDB ID:5Y3N) with ZINC05297837, ZINC05434822 compounds showing binding interactions with aminoacids

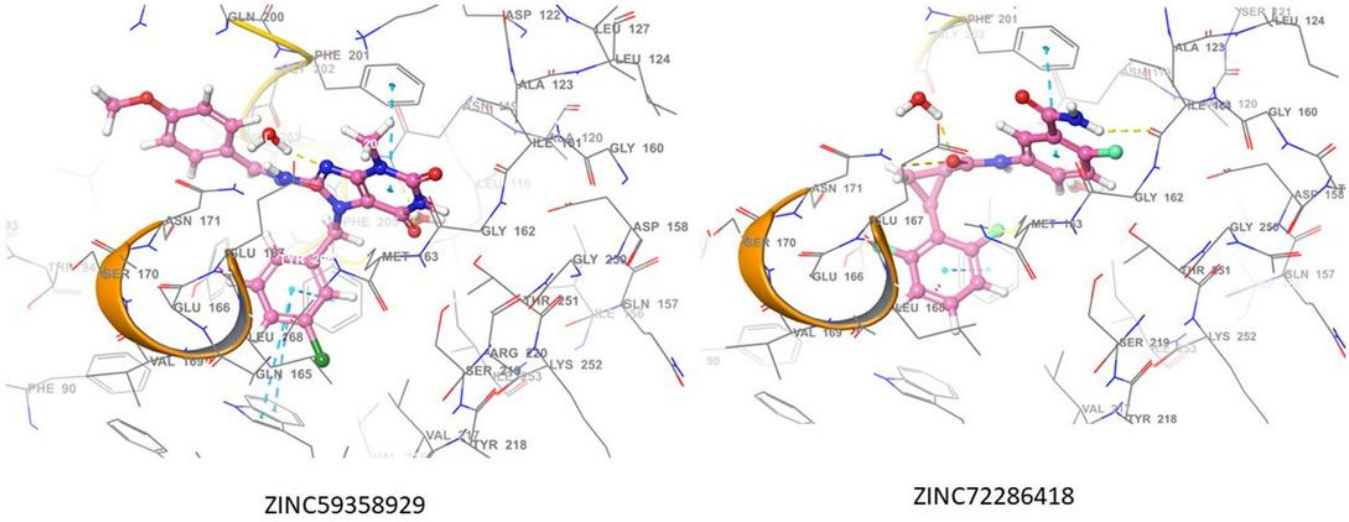

Figure 9

TRAP1(PDB ID:5Y3N) with compounds ZINC59358929, ZINC72286418, showing binding interactions with aminoacids

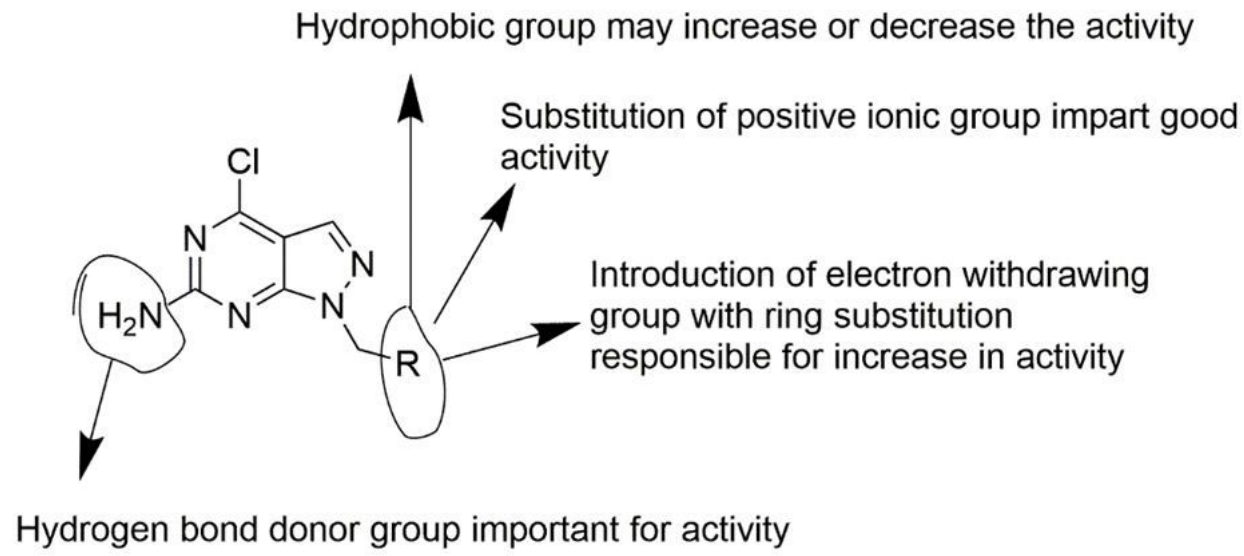

Figure 10

Ligand core with key features obtained by 3-D QSAR study for the development of novel molecules

Supplementary Files

This is a list of supplementary files associated with this preprint. Click to download.

- SupplementaryfileS3.xlsx
- SupplementaryfileS8.CSV
- SupplementaryfileS7.csv
- SupplementaryfileS6.CSV
- 17AAGGamitrinibTPP.JPG
- SupplementaryfileS5.csv
- 17AAGGamitrinibTPP1.JPG
- SupplementaryfileS4.csv
- SupplementaryfileS2.csv
- SupplementaryfileS1.csv